Probing Fundamental Physics with Gravitational Waves

Cyril Lagger

THE UNIVERSITY OF SYDNEY

CoEPP
ARC Centre of Excellence for Particle Physics at the Terascale

Seminar - Max-Planck-Institut für Kernphysik, Heidelberg - March 7, 2018

Overview

Gravitational Wave (GW) detection by LIGO/Virgo is promising for theoretical physics:

- confirms prediction of General Relativity
- allows to test GR (and its modifications) in a strong and dynamical regime
- suggests to look for other sources of GWs in relation to particle physics: phase transitions, cosmic strings,...

Overview

Gravitational Wave (GW) detection by LIGO/Virgo is promising for theoretical physics:

- confirms prediction of General Relativity
- allows to test GR (and its modifications) in a strong and dynamical regime
- suggests to look for other sources of GWs in relation to particle physics: phase transitions, cosmic strings,...

Two topics in this talk:

- constraining noncommutative space-time from LIGO/Virgo waveforms (transient signal)
- exploring beyond the Standard Model physics with GWs from phase transitions (stochastic background)

Part I: Test of GR and noncommutative space-time

First GW signal: GW150914

- Inspiral, merger and ring-down of a binary black hole observed by LIGO.
- Masses of $36^{+5}_{-4} M_\odot$ and $29^{+4}_{-4} M_\odot$.
- Frequency ranging from 35 to 250 Hz and velocity up to $\sim 0.5c$.

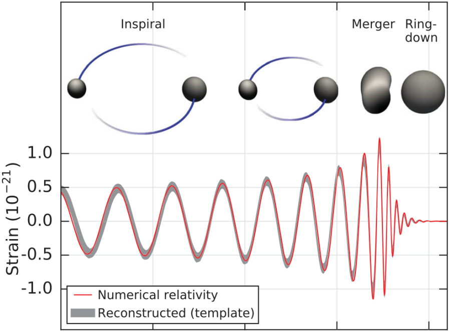

[LIGO/Virgo Coll., Phys. Rev. Lett. 116 (2016) 061102]

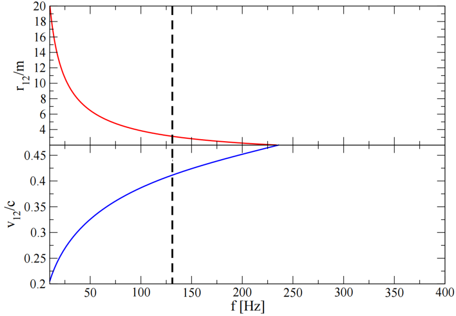

[N. Yunes, K. Yagi, F. Pretorius, arXiv:1603.08955]

An opportunity to test GR and its modifications

Einstein Field Equations (EFE) from GR predicts the waveform of such GWs :

- post-Newtonian formalism: analytical expansion in $\frac{v}{c}$ for the inspiralling
- numerical Relativity: accurate simulations including merger and ring-down

An opportunity to test GR and its modifications

Einstein Field Equations (EFE) from GR predicts the waveform of such GWs :

- post-Newtonian formalism: analytical expansion in $\frac{v}{c}$ for the inspiralling
- numerical Relativity: accurate simulations including merger and ring-down

GW150914 data are in good agreement with GR predictions

[LIGO/Virgo Coll., Phys. Rev. Lett. 116 (2016) 221101]

$\Rightarrow$ opportunity to test various models beyond GR.

[e.g.: N. Yunes, K. Yagi, F. Pretorius, arXiv:1603.08955, N. Yunes, E. Berti, K. Yagi, arXiv:1801.03208]

An opportunity to test GR and its modifications

Einstein Field Equations (EFE) from GR predicts the waveform of such GWs :

- post-Newtonian formalism: analytical expansion in $\frac{v}{c}$ for the inspiralling
- numerical Relativity: accurate simulations including merger and ring-down

GW150914 data are in good agreement with GR predictions

[LIGO/Virgo Coll., Phys. Rev. Lett. 116 (2016) 221101]

$\Rightarrow$ opportunity to test various models beyond GR.

[e.g.: N. Yunes, K. Yagi, F. Pretorius, arXiv:1603.08955, N. Yunes, E. Berti, K. Yagi, arXiv:1801.03208]

Our objective: constrain the scale of noncommutative space-time.

The post-Newtonian formalism

A perturbative approach to solve the EFE,

$$\Box h^{\alpha\beta} = \frac{16\pi G}{c^4}\tau^{\alpha\beta} \qquad \partial_\mu h^{\alpha\mu} = 0,$$

as an expansion in $\frac{v}{c}$. [L. Blanchet, Living Rev. Rel. 17 (2014)]

A perturbative approach to solve the EFE,

$$\Box h^{\alpha\beta} = \frac{16\pi G}{c^4}\tau^{\alpha\beta} \qquad \partial_\mu h^{\alpha\mu} = 0,$$

as an expansion in $\frac{v}{c}$. [L. Blanchet, Living Rev. Rel. 17 (2014)]

Notation:

- gravitational-field amplitude: $h^{\alpha\beta} = \sqrt{-g}g^{\alpha\beta} - \eta^{\alpha\beta}$
- matter-gravitational source: $\tau^{\alpha\beta} = |g|T^{\alpha\beta} + \frac{c^4}{16\pi G}\Lambda^{\alpha\beta}$
- $\mathcal{O}\left(n\right) \equiv \mathcal{O}\left(\frac{v^n}{c^n}\right)$

Far zone vs near zone

Iterative expansions in the near and far zones and matching strategy in the overlap zone:

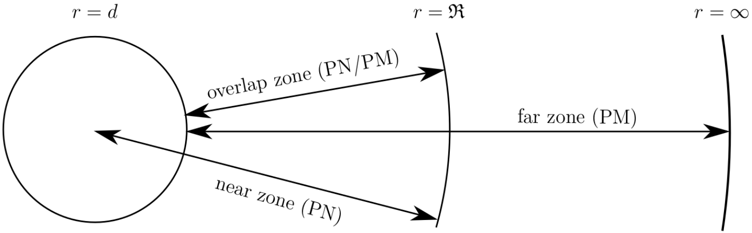

Far zone vs near zone

Iterative expansions in the near and far zones and matching strategy in the overlap zone:

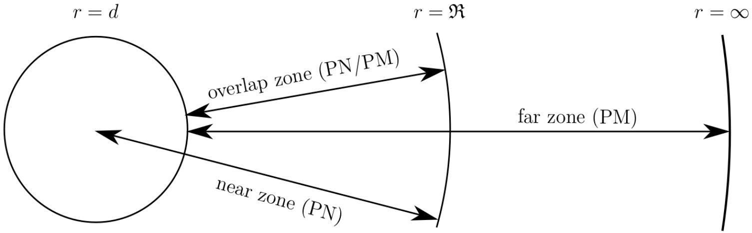

Post Minkowskian (PM) - G^n:

- $h^{\alpha\beta} = \sum_{n=1}^{\infty} G^n h_n^{\alpha\beta}$
- $\Box h^{\alpha\beta} = \Lambda^{\alpha\beta}$
- $\Box h_n^{\alpha\beta} = \Lambda_n^{\alpha\beta}[h_1, \cdots, h_{n-1}]$

Far zone vs near zone

Iterative expansions in the near and far zones and matching strategy in the overlap zone:

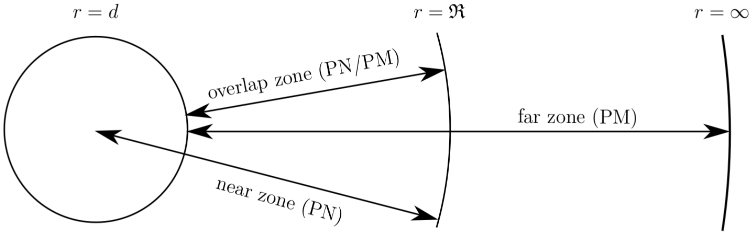

Post Newtonian (PN) - $\left(\frac{1}{c}\right)^n$:

- $h^{\alpha\beta} = \sum_{n=2}^{\infty} \frac{1}{c^n} h_n^{\alpha\beta}$
- $\tau^{\alpha\beta} = \sum_{n=-2}^{\infty} \frac{1}{c^n} \tau_n^{\alpha\beta}$
- $\nabla^2 h_n^{\alpha\beta} = 16\pi G\, \tau_{n-4}^{\alpha\beta} + \partial_t^2 h_{n-2}^{\alpha\beta}$

Post Minkowskian (PM) - G^n:

- $h^{\alpha\beta} = \sum_{n=1}^{\infty} G^n h_n^{\alpha\beta}$
- $\Box h^{\alpha\beta} = \Lambda^{\alpha\beta}$
- $\Box h_n^{\alpha\beta} = \Lambda_n^{\alpha\beta}[h_1, \cdots, h_{n-1}]$

Matter source

Consider a binary system of two black holes of masses m_1 and m_2. Usually approximated by two point-like particles:

$$T^{\mu\nu}(\mathbf{x}, t) = \frac{m_1}{\sqrt{g g_{\rho\sigma} \frac{v_1^\rho v_1^\sigma}{c^2}}} \, v_1^\mu(t) v_1^\nu(t) \; \delta^3(\mathbf{x} - \mathbf{y}_1(t)) + 1 \leftrightarrow 2$$

Matter source

Consider a binary system of two black holes of masses m_1 and m_2. Usually approximated by two point-like particles:

$$T^{\mu\nu}(\mathbf{x},t) = \frac{m_1}{\sqrt{g g_{\rho\sigma} \frac{v_1^\rho v_1^\sigma}{c^2}}} \, v_1^\mu(t) v_1^\nu(t) \; \delta^3(\mathbf{x} - \mathbf{y}_1(t)) + 1 \leftrightarrow 2$$

Useful parametrization:

- total mass: $M = m_1 + m_2$
- reduced mass: $\mu = \frac{m_1 m_2}{M}$
- symmetric mass ratio: $\nu = \frac{\mu}{M} = \frac{m_1 m_2}{M^2}$

Consider a binary system of two black holes of masses m_1 and m_2. Usually approximated by two point-like particles:

$$T^{\mu\nu}(\mathbf{x},t) = \frac{m_1}{\sqrt{g g_{\rho\sigma} \frac{v_1^\rho v_1^\sigma}{c^2}}} \, v_1^\mu(t) v_1^\nu(t) \; \delta^3(\mathbf{x} - \mathbf{y}_1(t)) + 1 \leftrightarrow 2$$

Useful parametrization:

- total mass: $M = m_1 + m_2$
- reduced mass: $\mu = \frac{m_1 m_2}{M}$
- symmetric mass ratio: $\nu = \frac{\mu}{M} = \frac{m_1 m_2}{M^2}$

We neglect spin effects in our considerations.

The balance equation

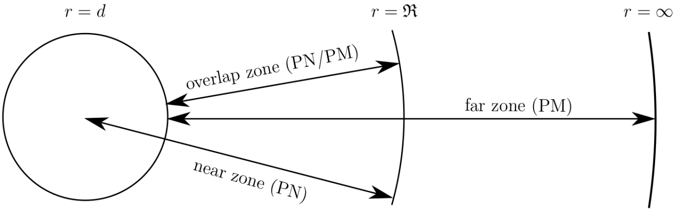

The balance equation

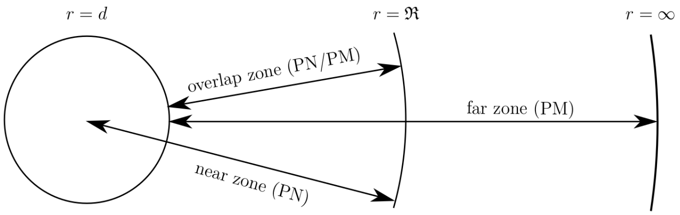

Equations of motion - energy E:

- $\nabla_\nu T^{\mu\nu} = 0$
- $\mathbf{a}_1 = -\frac{Gm_2}{r_{12}^2}\mathbf{n}_{12} + \mathcal{O}(2)$
- $E = \frac{m_1 v_1^2}{2} - \frac{Gm_1 m_2}{2r_{12}} + \mathcal{O}(2) + 1 \leftrightarrow 2$

The balance equation

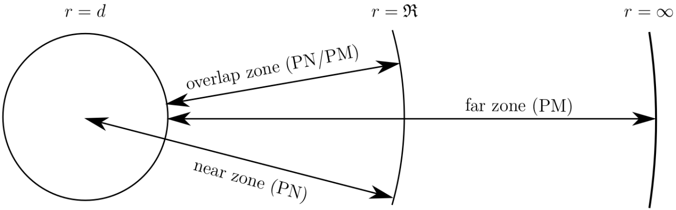

Equations of motion - energy E:

- $\nabla_\nu T^{\mu\nu} = 0$
- $\mathbf{a}_1 = -\frac{G m_2}{r_{12}^2}\mathbf{n}_{12} + \mathcal{O}(2)$
- $E = \frac{m_1 v_1^2}{2} - \frac{G m_1 m_2}{2 r_{12}} + \mathcal{O}(2) + 1 \leftrightarrow 2$

Radiated flux $\mathcal{F}$:

- $\mathcal{F} = \frac{G}{c^5}\left(\frac{1}{5} I_{ij}^{(3)} I_{ij}^{(3)} + \mathcal{O}(2)\right)$
- $\mathcal{F} = \frac{G}{c^5}\left(\frac{32 G^3 M^5 \nu^2}{5 r^5} + \mathcal{O}(2)\right)$

The balance equation

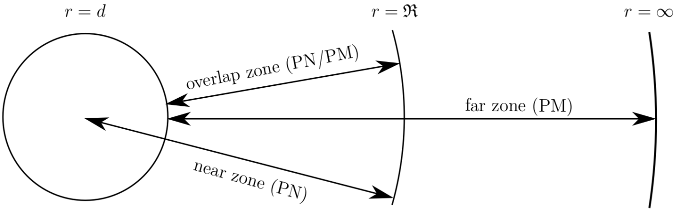

Equations of motion - energy E:

- $\nabla_\nu T^{\mu\nu} = 0$
- $\mathbf{a}_1 = -\frac{G m_2}{r_{12}^2} \mathbf{n}_{12} + \mathcal{O}(2)$
- $E = \frac{m_1 v_1^2}{2} - \frac{G m_1 m_2}{2 r_{12}} + \mathcal{O}(2) + 1 \leftrightarrow 2$

Radiated flux $\mathcal{F}$:

- $\mathcal{F} = \frac{G}{c^5} \left(\frac{1}{5} I_{ij}^{(3)} I_{ij}^{(3)} + \mathcal{O}(2) \right)$
- $\mathcal{F} = \frac{G}{c^5} \left(\frac{32 G^3 M^5 \nu^2}{5 r^5} + \mathcal{O}(2) \right)$

Conservation of energy implies the balance equation and the orbital phase:

$$\frac{dE}{dt} = -\mathcal{F} \quad \Rightarrow \quad \phi = \int \Omega(t) dt$$

State-of-the-art computations

For data analysis, consider the waveform in frequency space:

$$h(f) = A(f)\, e^{i\psi(f)}.$$

State-of-the-art computations

For data analysis, consider the waveform in frequency space:

$$h(f) = A(f)\, e^{i\psi(f)}.$$

The phase $\psi(f)$ (Fourier transform of $\phi(t)$) has been calculated to 3.5PN accuracy:

$$\psi(f) = 2\pi f t_c - \phi_c - \frac{\pi}{4} + \frac{3}{128} \sum_{j=0}^{7} \varphi_j \left(\frac{\pi M G f}{c^3} \right)^{(j-5)/3},$$

State-of-the-art computations

For data analysis, consider the waveform in frequency space:

$$h(f) = A(f)\, e^{i\psi(f)}.$$

The phase $\psi(f)$ (Fourier transform of $\phi(t)$) has been calculated to 3.5PN accuracy:

$$\psi(f) = 2\pi f t_c - \phi_c - \frac{\pi}{4} + \frac{3}{128} \sum_{j=0}^{7} \varphi_j \left(\frac{\pi M G f}{c^3} \right)^{(j-5)/3},$$

where the phase coefficients are

$$\begin{aligned}
\varphi_0 &= 1 \\
\varphi_1 &= 0 \\
\varphi_2 &= \tfrac{3715}{756} + \tfrac{55}{9}\nu \\
\varphi_3 &= -16\pi \\
\varphi_4 &= \tfrac{15293365}{508032} + \tfrac{27145}{504}\nu + \tfrac{3085}{72}\nu^2 \\
&\dots
\end{aligned}$$

[T. Damour, B. Iyer and B. Sathyaprakash, Phys. Rev. D 63 (2001) 044023]

[G. Faye, S. Marsat, L. Blanchet, B. Iyer, Class. Quantum Grav. 29 (2012) 175004]

GR vs GW150914: bayesian analysis

waveform regime	parameter	$f-$dependence	median single	median multiple	GR quantile single	GR quantile multiple	$\log_{10} B^{GR}_{model}$ single	$\log_{10} B^{GR}_{model}$ multiple
early-inspiral regime	$\delta\hat{\varphi}_0$	$f^{-5/3}$	$-0.1^{+0.1}_{-0.1}$	$1.3^{+3.0}_{-3.2}$	0.94	0.30	1.9 ± 0.2	3.7 ± 0.6
	$\delta\hat{\varphi}_1$	$f^{-4/3}$	$0.3^{+0.4}_{-0.4}$	$-0.5^{+0.6}_{-0.6}$	0.16	0.93	1.6 ± 0.2	
	$\delta\hat{\varphi}_2$	f^{-1}	$-0.4^{+0.3}_{-0.4}$	$-1.6^{+18.8}_{-16.6}$	0.96	0.56	1.2 ± 0.2	
	$\delta\hat{\varphi}_3$	$f^{-2/3}$	$0.2^{+0.2}_{-0.2}$	$2.0^{+13.4}_{-13.9}$	0.02	0.42	1.2 ± 0.2	
	$\delta\hat{\varphi}_4$	$f^{-1/3}$	$-1.9^{+1.6}_{-1.7}$	$-1.9^{+19.3}_{-16.4}$	0.98	0.56	0.3 ± 0.2	
	$\delta\hat{\varphi}_{5l}$	$\log(f)$	$0.8^{+0.5}_{-0.6}$	$-1.4^{+18.6}_{-16.9}$	0.01	0.55	0.7 ± 0.4	
	$\delta\hat{\varphi}_6$	$f^{1/3}$	$-1.4^{+1.1}_{-1.1}$	$1.2^{+16.8}_{-18.9}$	0.99	0.47	0.4 ± 0.2	
	$\delta\hat{\varphi}_{6l}$	$f^{1/3}\log(f)$	$8.9^{+6.8}_{-6.8}$	$-1.9^{+19.1}_{-16.1}$	0.02	0.57	-0.3 ± 0.2	
	$\delta\hat{\varphi}_7$	$f^{2/3}$	$3.8^{+2.9}_{-2.9}$	$3.2^{+15.1}_{-19.2}$	0.02	0.41	-0.0 ± 0.2	
intermediate regime	$\delta\hat{\beta}_2$	$\log f$	$0.1^{+0.4}_{-0.3}$	$0.2^{+0.6}_{-0.5}$	0.24	0.28	1.4 ± 0.2	2.3 ± 0.2
	$\delta\hat{\beta}_3$	f^{-3}	$0.1^{+0.6}_{-0.3}$	$-0.0^{+0.8}_{-0.7}$	0.31	0.56	1.2 ± 0.4	
merger-ringdown regime	$\delta\hat{\alpha}_2$	f^{-1}	$-0.1^{+0.4}_{-0.4}$	$0.0^{+1.0}_{-1.2}$	0.68	0.50	1.2 ± 0.2	2.1 ± 0.4
	$\delta\hat{\alpha}_3$	$f^{3/4}$	$-0.3^{+1.9}_{-1.5}$	$0.0^{+4.4}_{-4.4}$	0.60	0.51	0.7 ± 0.2	
	$\delta\hat{\alpha}_4$	$\tan^{-1}(af+b)$	$-0.1^{+0.5}_{-0.5}$	$-0.1^{+1.1}_{-1.0}$	0.68	0.62	1.1 ± 0.2	

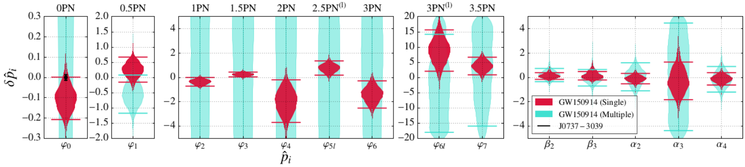

[LIGO/Virgo Coll., Phys. Rev. Lett. 116 (2016) 221101]

Noncommutative corrections to the waveform

A. Kobakhidze, CL, A. Manning, PRD 94 (2016) 064033

Noncommutative space-time

NC space-time arises in a number of contexts:

- Originally proposed by Heisenberg as an effective UV cutoff.
- Several formalisations (e.g. Snyder [Phys. Rev. 71 (1947) 38]).
- Noncommutative geometry [A. Connes, Inst. Hautes Etudes Sci. Publ. Math. 62 (1985) 257].
- Low-energy limit of string theory [N. Seiberg and E.Witten, JHEP 9909 (1999) 032].

Noncommutative space-time

NC space-time arises in a number of contexts:

- Originally proposed by Heisenberg as an effective UV cutoff.
- Several formalisations (e.g. Snyder [Phys. Rev. 71 (1947) 38]).
- Noncommutative geometry [A. Connes, Inst. Hautes Etudes Sci. Publ. Math. 62 (1985) 257].
- Low-energy limit of string theory [N. Seiberg and E.Witten, JHEP 9909 (1999) 032].

We focus on the canonical algebra of coordinates:

$$[\hat{x}^\mu, \hat{x}^\nu] = i\theta^{\mu\nu} \qquad \Delta x^\mu \Delta x^\nu \geq \frac{1}{2}|\theta^{\mu\nu}|$$

with noncommutative QFT - fields product replaced by Moyal product:

$$f(x) \star g(x) = f(x)g(x) + \sum_{n=1}^{+\infty} \left(\frac{i}{2}\right)^n \frac{1}{n!} \theta^{\alpha_1 \beta 1} \cdots \theta^{\alpha_n \beta_n} \partial_{\alpha_1} \cdots \partial_{\alpha_n} f(x) \, \partial_{\beta_1} \cdots \partial_{\beta_n} g(x)$$

Noncommutative space-time

NC space-time arises in a number of contexts:

- Originally proposed by Heisenberg as an effective UV cutoff.
- Several formalisations (e.g. Snyder [Phys. Rev. 71 (1947) 38]).
- Noncommutative geometry [A. Connes, Inst. Hautes Etudes Sci. Publ. Math. 62 (1985) 257].
- Low-energy limit of string theory [N. Seiberg and E.Witten, JHEP 9909 (1999) 032].

We focus on the canonical algebra of coordinates:

$$[\hat{x}^\mu, \hat{x}^\nu] = i\theta^{\mu\nu} \qquad \Delta x^\mu \Delta x^\nu \geq \frac{1}{2}|\theta^{\mu\nu}|$$

with noncommutative QFT - fields product replaced by Moyal product:

$$f(x) \star g(x) = f(x)g(x) + \sum_{n=1}^{+\infty} \left(\frac{i}{2}\right)^n \frac{1}{n!} \theta^{\alpha_1 \beta 1} \cdots \theta^{\alpha_n \beta_n} \partial_{\alpha_1} \cdots \partial_{\alpha_n} f(x) \partial_{\beta_1} \cdots \partial_{\beta_n} g(x)$$

Previous constraints on NC scale $|\theta|$ only at inverse $\sim$ TeV.

[S. Carroll et al., Phys. Rev. Lett.87 (2001) 141601] [X. Calmet, Eur. Phys. J. C41 (2005) 269]

Noncommutative effects on GWs

Expect modifications on both matter source and field equations.

Expect modifications on both matter source and field equations.

- Consider a Schwarzschild black hole described by a massive scalar field in noncommutative QFT [A. Kobakhidze, Phys. Rev. D79 (2009) 047701]:

$$T^{\mu\nu}_{NC}(x) = \frac{1}{2}\left(\partial^\mu\phi\star\partial^\nu\phi + \partial^\nu\phi\star\partial^\mu\phi\right) - \frac{1}{2}\eta^{\mu\nu}\left(\partial_\rho\phi\star\partial^\rho\phi - m^2\phi\star\phi\right)$$

Similar approach as for the quantum corrections of a Schwarzschild BH.

[N. E. J. Bjerrum-Bohr, J. F. Donoghue, B. R. Holstein, Phys. Rev. D68 (2003) 084005]

Noncommutative effects on GWs

Expect modifications on both matter source and field equations.

- Consider a Schwarzschild black hole described by a massive scalar field in noncommutative QFT[A. Kobakhidze, Phys. Rev. D79 (2009) 047701]:

$$T^{\mu\nu}_{NC}(x) = \frac{1}{2}\left(\partial^\mu\phi\star\partial^\nu\phi+\partial^\nu\phi\star\partial^\mu\phi\right)-\frac{1}{2}\eta^{\mu\nu}\left(\partial_\rho\phi\star\partial^\rho\phi-m^2\phi\star\phi\right)$$

  Similar approach as for the quantum corrections of a Schwarzschild BH.

  [N. E. J. Bjerrum-Bohr, J. F. Donoghue, B. R. Holstein, Phys. Rev. D68 (2003) 084005]

- Neglect corrections on the EFE since noncommutative gravity appears at $\mathcal{O}(|\theta|^2)$ and is model-dependent.

  [X. Calmet, A. Kobakhidze, Phys. Rev. D74 (2006) 047702] [P. Mukherjee, A. Saha, Phys. Rev. D74 (2006) 027702]

Energy-momentum tensor in noncommutative space-time

After quantising and keeping leading-order corrections of the Moyal product:

$$T^{\mu\nu}_{NC}(\mathbf{x},t) \approx T^{\mu\nu}_{GR}(\mathbf{x},t) + \frac{m^3G^2}{8c^4} v^\mu v^\nu \Theta^{kl} \partial_k \partial_l \, \delta^3(\mathbf{x} - \mathbf{y}(t))$$

with

$$\Theta^{kl} = \frac{\theta^{0k}\theta^{0l}}{l_P^2 t_P^2} + 2\frac{v_p}{c}\frac{\theta^{0k}\theta^{pl}}{l_P^3 t_P} + \frac{v_p v_q}{c^2}\frac{\theta^{kp}\theta^{lq}}{l_P^4} = \frac{\theta^{0k}\theta^{0l}}{l_P^2 t_P^2} + \mathcal{O}(1)$$

After quantising and keeping leading-order corrections of the Moyal product:

$$T^{\mu\nu}_{NC}(\mathbf{x},t) \approx T^{\mu\nu}_{GR}(\mathbf{x},t) + \frac{m^3G^2}{8c^4} v^\mu v^\nu \Theta^{kl} \partial_k \partial_l \, \delta^3(\mathbf{x} - \mathbf{y}(t))$$

with

$$\Theta^{kl} = \frac{\theta^{0k}\theta^{0l}}{l_P^2 t_P^2} + 2\frac{v_p}{c}\frac{\theta^{0k}\theta^{pl}}{l_P^3 t_P} + \frac{v_p v_q}{c^2}\frac{\theta^{kp}\theta^{lq}}{l_P^4} = \frac{\theta^{0k}\theta^{0l}}{l_P^2 t_P^2} + \mathcal{O}(1)$$

Binary black hole EMT with 2PN noncommutative corrections:

$$T^{\mu\nu}(\mathbf{x},t) = m_1\gamma_1 v_1^\mu v_1^\nu \delta^3(\mathbf{x} - \mathbf{y}_1(t)) + \frac{m_1^3 G^2 \kappa^2}{8c^4} v_1^\mu v_1^\nu \theta^k \theta^l \partial_k \partial_l \, \delta^3(\mathbf{x} - \mathbf{y}_1(t)) + 1 \leftrightarrow 2$$

where

$$\kappa\theta^i = \frac{\theta^{0i}}{l_P t_P}.$$

Noncommutative effects on gravitational waveform

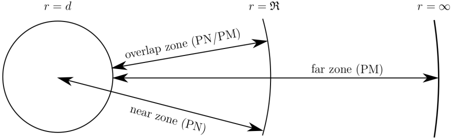

$$\frac{d(E_{GR}+E_{NC})}{dt} = -\mathcal{F}_{NC} - \mathcal{F}_{NC}$$

Noncommutative effects on gravitational waveform

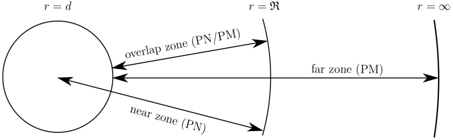

$$\frac{d(E_{GR}+E_{NC})}{dt} = -\mathcal{F}_{NC} - \mathcal{F}_{NC}$$

Lowest-order corrections appear at 2PN:

$$E_{NC} = -\frac{3M^3\mu(1-2\nu)G^3\kappa^2}{8c^4r^3}\theta^k\theta^l\hat{n}_{kl} + \mathcal{O}(5)$$

$$\mathcal{F}_{NC} = \frac{G}{c^5}\left(-\frac{36}{5}\frac{G^5M^7}{c^4r^7}\nu^2(1-2\nu)\kappa^2 + \mathcal{O}(5)\right)$$

Noncommutative effects on gravitational waveform

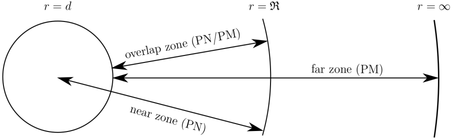

$$\frac{d(E_{GR} + E_{NC})}{dt} = -\mathcal{F}_{NC} - \mathcal{F}_{NC}$$

Lowest-order corrections appear at 2PN:

$$E_{NC} = -\frac{3M^3\mu(1-2\nu)G^3\kappa^2}{8c^4r^3}\theta^k\theta^l\hat{n}_{kl} + \mathcal{O}(5)$$

$$\mathcal{F}_{NC} = \frac{G}{c^5}\left(-\frac{36}{5}\frac{G^5M^7}{c^4r^7}\nu^2(1-2\nu)\kappa^2 + \mathcal{O}(5)\right)$$

Lowest order modification to the waveform phase:

$$\varphi_4 = \frac{15293365}{508032} + \frac{27145}{504}\nu + \frac{3085}{72}\nu^2 + \frac{5}{4}(1-2\nu)\kappa^2$$

Noncommutativity vs GW150914

waveform regime	parameter	f−dependence	median single	median multiple	GR quantile single	GR quantile multiple	$\log_{10} B^{GR}_{model}$ single	$\log_{10} B^{GR}_{model}$ multiple
early-inspiral regime	$\delta\hat{\varphi}_0$	$f^{-5/3}$	$-0.1^{+0.1}_{-0.1}$	$1.3^{+3.0}_{-3.2}$	0.94	0.30	1.9 ± 0.2	3.7 ± 0.6
	$\delta\hat{\varphi}_1$	$f^{-4/3}$	$0.3^{+0.4}_{-0.4}$	$-0.5^{+0.6}_{-0.6}$	0.16	0.93	1.6 ± 0.2	
	$\delta\hat{\varphi}_2$	f^{-1}	$-0.4^{+0.3}_{-0.4}$	$-1.6^{+18.8}_{-16.6}$	0.96	0.56	1.2 ± 0.2	
	$\delta\hat{\varphi}_3$	$f^{-2/3}$	$0.2^{+0.2}_{-0.2}$	$2.0^{+13.4}_{-13.9}$	0.02	0.42	1.2 ± 0.2	
	$\delta\hat{\varphi}_4$	$f^{-1/3}$	$-1.9^{+1.6}_{-1.7}$	$-1.9^{+19.3}_{-16.4}$	0.98	0.56	0.3 ± 0.2	
	$\delta\hat{\varphi}_{5l}$	$\log(f)$	$0.8^{+0.5}_{-0.6}$	$-1.4^{+18.6}_{-16.9}$	0.01	0.55	0.7 ± 0.4	
	$\delta\hat{\varphi}_6$	$f^{1/3}$	$-1.4^{+1.1}_{-1.1}$	$1.2^{+16.8}_{-18.9}$	0.99	0.47	0.4 ± 0.2	
	$\delta\hat{\varphi}_{6l}$	$f^{1/3}\log(f)$	$8.9^{+6.8}_{-6.8}$	$-1.9^{+19.1}_{-16.1}$	0.02	0.57	-0.3 ± 0.2	
	$\delta\hat{\varphi}_7$	$f^{2/3}$	$3.8^{+2.9}_{-2.9}$	$3.2^{+15.1}_{-19.2}$	0.02	0.41	-0.0 ± 0.2	
intermediate regime	$\delta\hat{\beta}_2$	$\log f$	$0.1^{+0.4}_{-0.3}$	$0.2^{+0.6}_{-0.5}$	0.24	0.28	1.4 ± 0.2	2.3 ± 0.2
	$\delta\hat{\beta}_3$	f^{-3}	$0.1^{+0.6}_{-0.3}$	$-0.0^{+0.8}_{-0.7}$	0.31	0.56	1.2 ± 0.4	
merger-ringdown regime	$\delta\hat{\alpha}_2$	f^{-1}	$-0.1^{+0.4}_{-0.4}$	$0.0^{+1.0}_{-1.2}$	0.68	0.50	1.2 ± 0.2	2.1 ± 0.4
	$\delta\hat{\alpha}_3$	$f^{3/4}$	$-0.3^{+1.9}_{-1.5}$	$0.0^{+4.4}_{-4.4}$	0.60	0.51	0.7 ± 0.2	
	$\delta\hat{\alpha}_4$	$\tan^{-1}(af+b)$	$-0.1^{+0.5}_{-0.5}$	$-0.1^{+1.1}_{-1.0}$	0.68	0.62	1.1 ± 0.2	

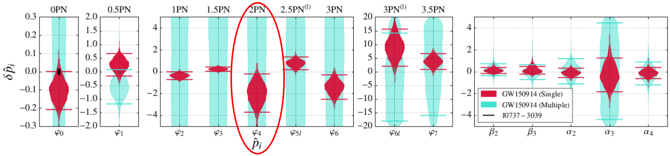

$$\delta\varphi_4^{NC} = \frac{\varphi_4^{NC}}{\varphi_4^{GR}} = \frac{1270080\,(1-2\nu)}{4353552\,\nu^2 + 5472432\,\nu + 3058673}\kappa^2$$

$$|\delta\varphi_4^{NC}| \lesssim 20 \Rightarrow \sqrt{\kappa} \lesssim 3.5$$

Summary of Part I

- Several observations of binary system merger by LIGO/Virgo

Summary of Part I

- Several observations of binary system merger by LIGO/Virgo
- GW waveform consistent with GR

Summary of Part I

- Several observations of binary system merger by LIGO/Virgo
- GW waveform consistent with GR
- Explicit computation of the lowest-order (2PN) noncommutative correction to the GW waveform.

Summary of Part I

- Several observations of binary system merger by LIGO/Virgo
- GW waveform consistent with GR
- Explicit computation of the lowest-order (2PN) noncommutative correction to the GW waveform.
- Constraint on the scale of noncommutativity to around the Planck scale:

$$|\theta^{0i}| \lesssim \mathcal{O}(10) \cdot l_P t_P$$

Part II: Phase transitions and Gravitational Waves

First-order phase transition and GWs

Hot Big Bang scenario:

- early Universe $\sim$ hot plasma (high T)
- scalar field(s) behaviour dictated by their free energy density $\mathcal{F}(\rho, T)$
- dynamics depend on the underlying particle physics model

2nd-order transition / crossover:

- smooth dynamics
- no GWs

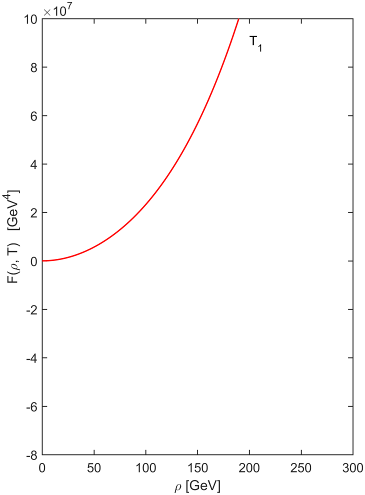

First-order phase transition and GWs

Hot Big Bang scenario:

- early Universe $\sim$ hot plasma (high T)
- scalar field(s) behaviour dictated by their free energy density $\mathcal{F}(\rho, T)$
- dynamics depend on the underlying particle physics model

2nd-order transition / crossover:

- smooth dynamics
- no GWs

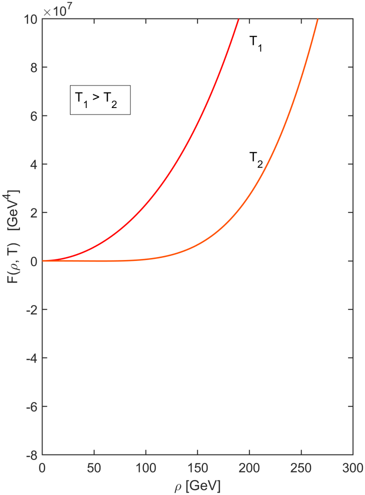

First-order phase transition and GWs

Hot Big Bang scenario:

- early Universe $\sim$ hot plasma (high T)
- scalar field(s) behaviour dictated by their free energy density $\mathcal{F}(\rho, T)$
- dynamics depend on the underlying particle physics model

2nd-order transition / crossover:

- smooth dynamics
- no GWs

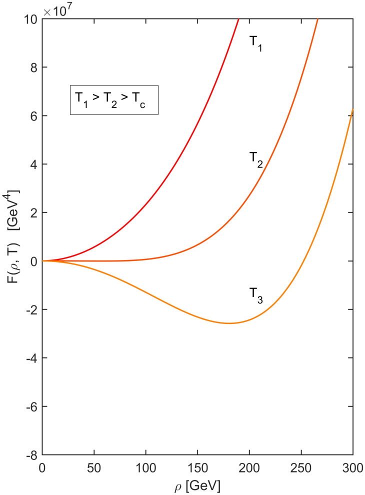

First-order phase transition and GWs

Hot Big Bang scenario:

- early Universe $\sim$ hot plasma (high T)
- scalar field(s) behaviour dictated by their free energy density $\mathcal{F}(\rho, T)$
- dynamics depend on the underlying particle physics model

2nd-order transition / crossover:

- smooth dynamics
- no GWs

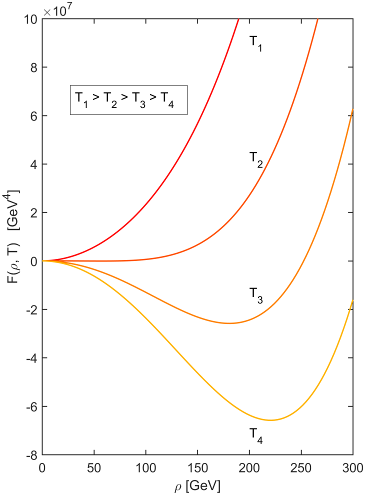

First-order phase transition and GWs

Hot Big Bang scenario:

- early Universe $\sim$ hot plasma (high T)
- scalar field(s) behaviour dictated by their free energy density $\mathcal{F}(\rho, T)$
- dynamics depend on the underlying particle physics model

1st-order transition:

- bubble nucleation
- bubble collision
- stochastic GW background

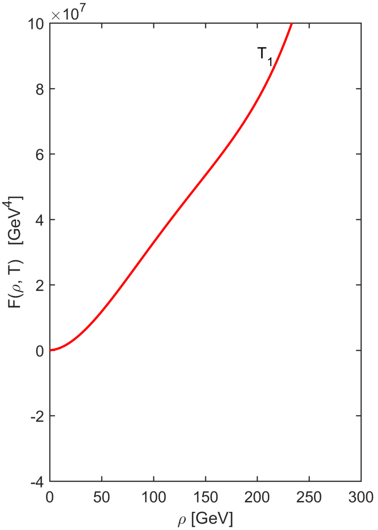

First-order phase transition and GWs

Hot Big Bang scenario:

- early Universe $\sim$ hot plasma (high T)
- scalar field(s) behaviour dictated by their free energy density $\mathcal{F}(\rho, T)$
- dynamics depend on the underlying particle physics model

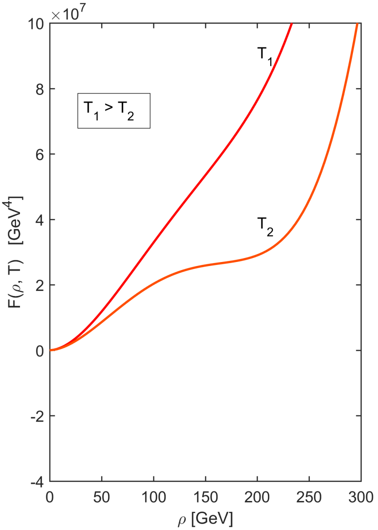

1st-order transition:

- bubble nucleation
- bubble collision
- stochastic GW background

First-order phase transition and GWs

Hot Big Bang scenario:

- early Universe $\sim$ hot plasma (high T)
- scalar field(s) behaviour dictated by their free energy density $\mathcal{F}(\rho, T)$
- dynamics depend on the underlying particle physics model

1st-order transition:

- bubble nucleation
- bubble collision
- stochastic GW background

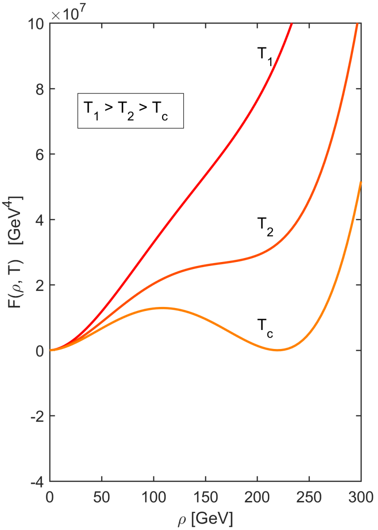

First-order phase transition and GWs

Hot Big Bang scenario:

- early Universe ∼ hot plasma (high T)
- scalar field(s) behaviour dictated by their free energy density $\mathcal{F}(\rho, T)$
- dynamics depend on the underlying particle physics model

1st-order transition:

- bubble nucleation
- bubble collision
- stochastic GW background

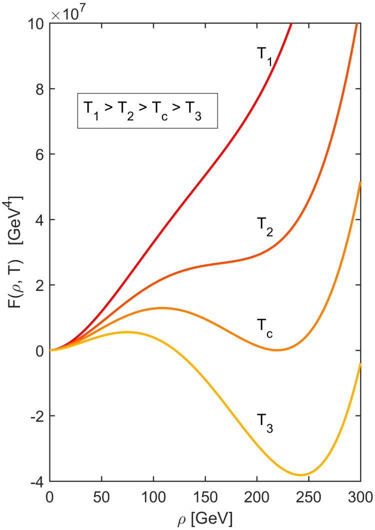

Example of a very recent simulation

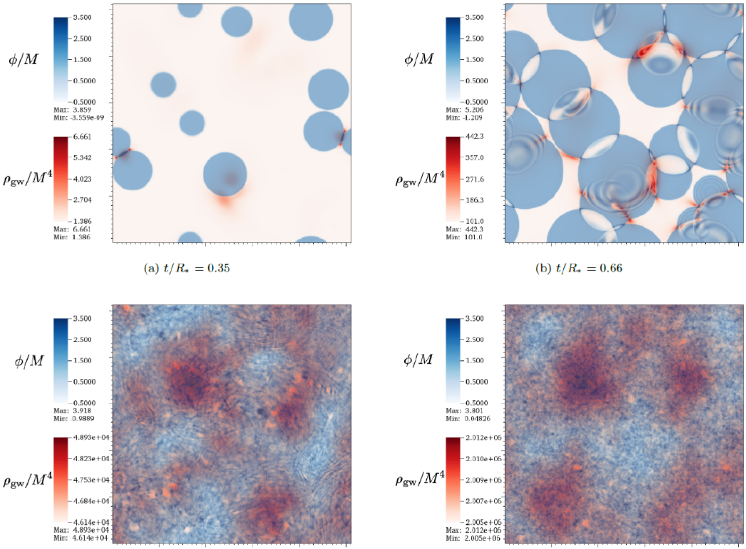

(a) $t/R_* = 0.35$

(b) $t/R_* = 0.66$

(c) $t/R_* = 2.50$

(d) $t/R_* = 7.8$

[D. Cutting, M. Hindmarsh, D. Weir, arXiv:1802.05712]

Looking for BSM physics with GWs

A possible probe of new physics:

- no 1st-order PT in the Standard Model [K. Kajantie et al., Phys. Rev. Lett. 77 (1996) 2887]

  $\Rightarrow$ no stochastic GW background predicted in the SM

- various BSM models account for a 1st-order EWPT (e.g. motivated by electroweak baryogenesis)

Looking for BSM physics with GWs

A possible probe of new physics:

- no 1st-order PT in the Standard Model [K. Kajantie et al., Phys. Rev. Lett. 77 (1996) 2887]

  $\Rightarrow$ no stochastic GW background predicted in the SM

- various BSM models account for a 1st-order EWPT (e.g. motivated by electroweak baryogenesis)

Examples of models considered:

- non-linearly realised electroweak gauge group

  [A. Kobakhidze, A. Manning, J. Yue, arXiv:1607.00883] [A. Kobakhidze, CL, A. Manning, J. Yue, arXiv:1703.06552]

- Standard Model with hidden scale invariance

  [S. Arunasalam, A. Kobakhidze, CL, S. Liang, A. Zhou, arXiv:1709.10322]

Stochastic background from bubble collisions

Stochastic background from three sources [C. Caprini et al., JCAP 1604 (2016) no.04 001]:

$$h^2\Omega_{\mathrm{GW}}(f) \simeq h^2\Omega_{col} + h^2\Omega_{sw} + h^2\Omega_{\mathrm{MHD}}$$

Stochastic background from bubble collisions

Stochastic background from three sources [C. Caprini et al., JCAP 1604 (2016) no.04 001]:

$$h^2\Omega_{\text{GW}}(f) \simeq h^2\Omega_{col} + h^2\Omega_{sw} + h^2\Omega_{\text{MHD}}$$

Ω_{col} dominant for very strong PT (as considered here).

Stochastic background from bubble collisions

Stochastic background from three sources [C. Caprini et al., JCAP 1604 (2016) no.04 001]:

$$h^2\Omega_{\text{GW}}(f) \simeq h^2\Omega_{col} + h^2\Omega_{sw} + h^2\Omega_{\text{MHD}}$$

Ω_{col} dominant for very strong PT (as considered here).

Peak frequency and amplitude of the background mainly depend on the bubble size $\bar{R}$ at collision and kinetic energy ρ_{kin} stored in the bubbles:

- $f_{\text{peak}} \sim (\bar{R})^{-1}$
- $\Omega_{col} \sim (\bar{R}H_p)^2 \frac{\rho_{\text{kin}}^2}{(\rho_{\text{kin}}+\rho_{\text{rad}})^2}$

Bubble-collision simulations

Going beyond dimensional analysis with numerical simulations (and redshift)

[S. Huber and T. Konstandin, JCAP 0809 (2008) 022]

Bubble-collision simulations

Going beyond dimensional analysis with numerical simulations (and redshift)

[S. Huber and T. Konstandin, JCAP 0809 (2008) 022]

Notation: $\alpha = \rho_{\text{kin}} / \rho_{\text{rad}}$ and $\beta = v\bar{R}^{-1}$

Bubble-collision simulations

Going beyond dimensional analysis with numerical simulations (and redshift)

[S. Huber and T. Konstandin, JCAP 0809 (2008) 022]

Notation: $\alpha = \rho_{\mathsf{kin}}/\rho_{\mathsf{rad}}$ and $\beta = v\bar{R}^{-1}$

Amplitude:

$$h^2\Omega_{col}(f) = 1.67 \times 10^{-5}\left(\frac{100}{g_*}\right)^{1/3}\left(\frac{\beta}{H_p}\right)^{-2}\kappa_v^2\left(\frac{\alpha}{1+\alpha}\right)^2\left(\frac{0.11v^3}{0.42+v^2}\right)S(f)$$

$$S(f) = \frac{3.8(f/f_0)^{2.8}}{1+2.8(f/f_0)^{3.8}}$$

Bubble-collision simulations

Going beyond dimensional analysis with numerical simulations (and redshift)

[S. Huber and T. Konstandin, JCAP 0809 (2008) 022]

Notation: $\alpha = \rho_{\mathsf{kin}} / \rho_{\mathsf{rad}}$ and $\beta = v\bar{R}^{-1}$

Amplitude:

$$h^2\Omega_{col}(f) = 1.67 \times 10^{-5} \left(\frac{100}{g_*}\right)^{1/3} \left(\frac{\beta}{H_p}\right)^{-2} \kappa_v^2 \left(\frac{\alpha}{1+\alpha}\right)^2 \left(\frac{0.11 v^3}{0.42 + v^2}\right) S(f)$$

$$S(f) = \frac{3.8(f/f_0)^{2.8}}{1 + 2.8(f/f_0)^{3.8}}$$

Peak frequency:

$$f_0 = 1.65 \times 10^{-7} \left(\frac{T_p}{1\ \text{GeV}}\right) \left(\frac{g_*}{100}\right)^{1/6} H_p^{-1} \beta \left(\frac{0.62}{1.8 - 0.1v + v^2}\right) \text{Hz}$$

Bubble-collision simulations

Going beyond dimensional analysis with numerical simulations (and redshift)

[S. Huber and T. Konstandin, JCAP 0809 (2008) 022]

Notation: $\alpha = \rho_{\mathsf{kin}}/\rho_{\mathsf{rad}}$ and $\beta = v\bar{R}^{-1}$

Amplitude:

$$h^2\Omega_{col}(f) = 1.67 \times 10^{-5} \left(\frac{100}{g_*}\right)^{1/3} \left(\frac{\beta}{H_p}\right)^{-2} \kappa_v^2 \left(\frac{\alpha}{1+\alpha}\right)^2 \left(\frac{0.11 v^3}{0.42 + v^2}\right) S(f)$$

$$S(f) = \frac{3.8(f/f_0)^{2.8}}{1 + 2.8(f/f_0)^{3.8}}$$

Peak frequency:

$$f_0 = 1.65 \times 10^{-7} \left(\frac{T_p}{1\ \mathrm{GeV}}\right) \left(\frac{g_*}{100}\right)^{1/6} H_p^{-1} \beta \left(\frac{0.62}{1.8 - 0.1v + v^2}\right) \mathrm{Hz}$$

The set of parameters $(\bar{R}, \rho_{\mathsf{kin}}, v, \kappa_v)$ is determined by the underlying particle physics model.

Different scenarios of electroweak phase transition

Typical case (quick PT):

- $\mathcal{O}(1)$ bubbles produced per Hubble volume at $T_n \lesssim T_{EW}$
- they rapidly collide $\Rightarrow$ percolation temperature $T_p \sim T_n$
- time scale of the process much shorter than Hubble time
- $f_{\text{peak}} \sim$ milliHertz $\Rightarrow$ range of LISA [C. Caprini et al., JCAP 1604 (2016) no.04 001]

Different scenarios of electroweak phase transition

Typical case (quick PT):

- $\mathcal{O}(1)$ bubbles produced per Hubble volume at $T_n \lesssim T_{EW}$
- they rapidly collide $\Rightarrow$ percolation temperature $T_p \sim T_n$
- time scale of the process much shorter than Hubble time
- $f_{\text{peak}} \sim$ milliHertz $\Rightarrow$ range of LISA [C. Caprini et al., JCAP 1604 (2016) no.04 001]

Prolonged and supercooled PT [A. Kobakhidze, CL, A. Manning, J. Yue, arXiv:1703.06552]:

- weaker nucleation probability
- less bubbles produced $\Rightarrow$ more time needed for them to collide
- $\Rightarrow T_p \ll T_n \lesssim T_{EW}$
- $f_{\text{peak}} \sim 10^{-8}$ Hertz $\Rightarrow$ range of Pulsar Timing Arrays

Different scenarios of electroweak phase transition

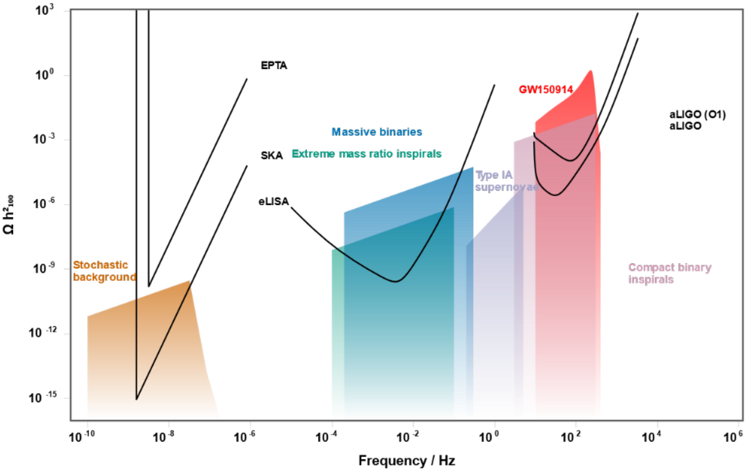

[From rhcole.com/apps/GWplotter/]

Prolonged electroweak phase transition

A. Kobakhidze, CL, A. Manning, J. Yue [Eur.Phys.J. C77 (2017), arXiv:1703.06552]

Realisation of $SU(2)_L \times U(1)_Y$

Main idea:

- $\mathcal{G}_{\mathsf{coset}} = SU(2)_L \times U(1)_Y / U(1)_Q$ is gauged
- with broken generators $T^i = \sigma^i - \delta^{i3}\mathbb{I}$ and Goldstone bosons $\pi^i(x)$
- physical Higgs as a singlet $\rho(x) \sim (\mathbf{1},\mathbf{1})_0$

Realisation of $SU(2)_L \times U(1)_Y$

Main idea:

- $\mathcal{G}_{\text{coset}} = SU(2)_L \times U(1)_Y / U(1)_Q$ is gauged
- with broken generators $T^i = \sigma^i - \delta^{i3}\mathbb{I}$ and Goldstone bosons $\pi^i(x)$
- physical Higgs as a singlet $\rho(x) \sim (\mathbf{1},\mathbf{1})_0$

SM Higgs doublet identified as $H(x) = \frac{\rho(x)}{\sqrt{2}} e^{\frac{i}{2}\pi^i(x) T^i} \begin{pmatrix} 0 \\ 1 \end{pmatrix}, \qquad i \in \{1,2,3\}$

Realisation of $SU(2)_L \times U(1)_Y$

Main idea:

- $\mathcal{G}_{\text{coset}} = SU(2)_L \times U(1)_Y / U(1)_Q$ is gauged
- with broken generators $T^i = \sigma^i - \delta^{i3}\mathbb{I}$ and Goldstone bosons $\pi^i(x)$
- physical Higgs as a singlet $\rho(x) \sim (\mathbf{1},\mathbf{1})_0$

SM Higgs doublet identified as $H(x) = \frac{\rho(x)}{\sqrt{2}} e^{\frac{i}{2}\pi^i(x) T^i} \begin{pmatrix} 0 \\ 1 \end{pmatrix}, \qquad i \in \{1,2,3\}$

SM particle content but BSM interactions

Realisation of $SU(2)_L \times U(1)_Y$

Main idea:

- $\mathcal{G}_{\text{coset}} = SU(2)_L \times U(1)_Y / U(1)_Q$ is gauged
- with broken generators $T^i = \sigma^i - \delta^{i3}\mathbb{I}$ and Goldstone bosons $\pi^i(x)$
- physical Higgs as a singlet $\rho(x) \sim (\mathbf{1}, \mathbf{1})_0$

SM Higgs doublet identified as $H(x) = \frac{\rho(x)}{\sqrt{2}} e^{\frac{i}{2}\pi^i(x) T^i} \begin{pmatrix} 0 \\ 1 \end{pmatrix}, \qquad i \in \{1,2,3\}$

SM particle content but BSM interactions

Minimal setup (usual SM configurations except Higgs potential):

$$V^{(0)}(\rho) = -\frac{\mu^2}{2}\rho^2 + \frac{\kappa}{3}\rho^3 + \frac{\lambda}{4}\rho^4.$$

Realisation of $SU(2)_L \times U(1)_Y$

Main idea:

- $\mathcal{G}_{\text{coset}} = SU(2)_L \times U(1)_Y / U(1)_Q$ is gauged
- with broken generators $T^i = \sigma^i - \delta^{i3}\mathbb{I}$ and Goldstone bosons $\pi^i(x)$
- physical Higgs as a singlet $\rho(x) \sim (\mathbf{1},\mathbf{1})_0$

SM Higgs doublet identified as $H(x) = \frac{\rho(x)}{\sqrt{2}} e^{\frac{i}{2}\pi^i(x)T^i} \begin{pmatrix} 0 \\ 1 \end{pmatrix}, \qquad i \in \{1,2,3\}$

SM particle content but BSM interactions

Minimal setup (usual SM configurations except Higgs potential):

$$V^{(0)}(\rho) = -\frac{\mu^2}{2}\rho^2 + \frac{\kappa}{3}\rho^3 + \frac{\lambda}{4}\rho^4.$$

For additional details, see e.g.: [M. Gonzalez-Alonso et al., Eur. Phys. J. C 75 (2015) 3, 128] [D. Binosi and A. Quadri, JHEP 1302 (2013) 020] [A. Kobakhidze, arXiv:1208.5180] [R. Contino et al., JHEP 1005 (2010) 089]

Tree-level potential

Model specified by one parameter: $\kappa = \bar{\kappa} \cdot \frac{m_h^2}{v} \sim 63.5 \cdot \bar{\kappa}$ GeV.

Barrier in the Higgs potential at tree level $\Rightarrow$ likely to allow a strong 1st-order EWPT.

Tree-level potential

Model specified by one parameter: $\kappa = \bar{\kappa} \cdot \frac{m_h^2}{v} \sim 63.5 \cdot \bar{\kappa}$ GeV.

Barrier in the Higgs potential at tree level $\Rightarrow$ likely to allow a strong 1st-order EWPT.

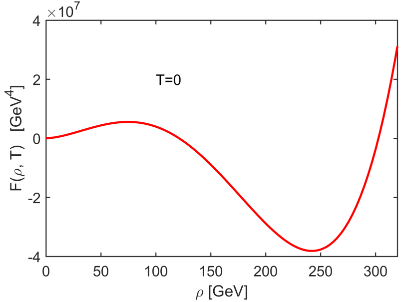

Bubble nucleation probability

Decay probability per unit volume per unit time: $\Gamma(T) \approx A(T)e^{-S(T)}$ [A. Linde, Nucl. Phys. B216 (1983) 421]

Bubble nucleation probability

Decay probability per unit volume per unit time: $\Gamma(T) \approx A(T) e^{-S(T)}$ [A. Linde, Nucl. Phys. B216 (1983) 421]

Computation of the Euclidean action:

$$S[\rho, T] = 4\pi \int_0^\beta d\tau \int_0^\infty dr\, r^2 \left[\frac{1}{2} \left(\frac{d\rho}{d\tau} \right)^2 + \frac{1}{2} \left(\frac{d\rho}{dr} \right)^2 + \mathcal{F}(\rho, T) \right]$$

$$\frac{\partial^2 \rho}{\partial \tau^2} + \frac{\partial^2 \rho}{\partial r^2} + \frac{2}{r} \frac{\partial \rho}{\partial r} - \frac{\partial \mathcal{F}}{\partial \rho}(\rho, T) = 0 \quad + \quad \text{boundary conditions}$$

$$S[\rho, T] \approx \begin{cases} S_4[\rho, T] = 2\pi^2 \int_0^\infty d\tilde{r}\, \tilde{r}^3 \left[\frac{1}{2} \left(\frac{d\rho}{d\tilde{r}} \right)^2 + \mathcal{F}(\rho, T) \right], & T \ll R_0^{-1} \\ \frac{1}{T} S_3[\rho, T] = \frac{4\pi}{T} \int_0^\infty dr\, r^2 \left[\frac{1}{2} \left(\frac{d\rho}{dr} \right)^2 + \mathcal{F}(\rho, T) \right], & T \gg R_0^{-1} \end{cases}$$

Bubble nucleation probability

Decay probability per unit volume per unit time: $\Gamma(T) \approx A(T)e^{-S(T)}$ [A. Linde, Nucl. Phys. B216 (1983) 421]

Some numerical results:

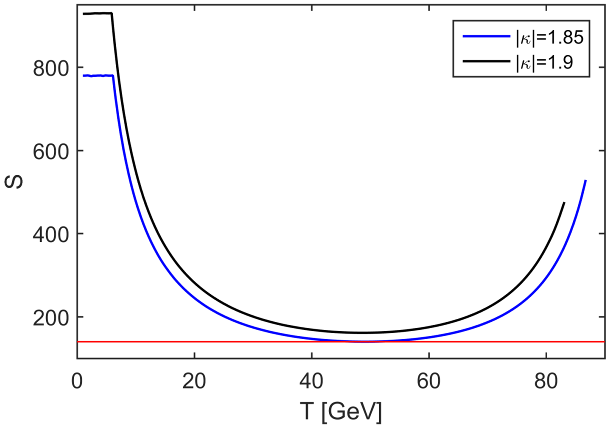

Standard scenario: number of bubbles $\sim \mathcal{O}(1)$ requires $\min S \lesssim 140$

Phase transition dynamics

General formalism in expanding universe: [M. Turner et al., Phys. Rev. D46 (1992) 2384].

Phase transition dynamics

General formalism in expanding universe: [M. Turner et al., Phys. Rev. D46 (1992) 2384].

Probability for a point of space-time to remain in the false-vacuum:

$$p(t) = \exp\left[-\frac{4\pi}{3}\int_{t_\star}^{t} dt'\Gamma(t')a^3(t')r^3(t,t')\right] \qquad r(t,t') = \int_{t'}^{t} dt'' \frac{v(t'')}{a(t'')}$$

Completion of the PT requires $p(t) \to 0$

Percolation temperature ($\sim$ collision) [L. Leitao et al., JCAP 1210 (2012) 024]: $p(t_p) \approx 0.7$

Phase transition dynamics

General formalism in expanding universe: [M. Turner et al., Phys. Rev. D46 (1992) 2384].

Probability for a point of space-time to remain in the false-vacuum:

$$p(t) = \exp\left[-\frac{4\pi}{3}\int_{t_\star}^{t} dt' \Gamma(t') a^3(t') r^3(t,t')\right] \qquad r(t,t') = \int_{t'}^{t} dt'' \frac{v(t'')}{a(t'')}$$

Completion of the PT requires $p(t) \to 0$

Percolation temperature ($\sim$ collision) [L. Leitao et al., JCAP 1210 (2012) 024]: $p(t_p) \approx 0.7$

Number density of produced bubbles:

$$\frac{dN}{dR}(t, t_R) = \Gamma(t_R)\left(\frac{a(t_R)}{a(t)}\right)^4 \frac{p(t_R)}{v(t_R)}$$

Phase transition dynamics

General formalism in expanding universe: [M. Turner et al., Phys. Rev. D46 (1992) 2384].

Probability for a point of space-time to remain in the false-vacuum:

$$p(t) = \exp\left[-\frac{4\pi}{3}\int_{t_\star}^{t} dt' \Gamma(t') a^3(t') r^3(t,t')\right] \qquad r(t,t') = \int_{t'}^{t} dt'' \frac{v(t'')}{a(t'')}$$

Completion of the PT requires $p(t) \to 0$

Percolation temperature ($\sim$ collision) [L. Leitao et al., JCAP 1210 (2012) 024]: $p(t_p) \approx 0.7$

Number density of produced bubbles:

$$\frac{dN}{dR}(t, t_R) = \Gamma(t_R) \left(\frac{a(t_R)}{a(t)}\right)^4 \frac{p(t_R)}{v(t_R)}$$

Nucleation temperature T_n: maximum of $\frac{dN}{dR}(t_p, t_R)$

Bubbles properties at collision

By definition:

- most bubbles collide at t_p
- majority of them produced at t_n

$\Rightarrow$ bubble physical radius: $\bar{R} = a(t_p) r(t_p, t_n)$

Bubbles properties at collision

By definition:

- most bubbles collide at t_p
- majority of them produced at t_n

$\Rightarrow$ bubble physical radius: $\bar{R} = a(t_p) r(t_p, t_n)$

Kinetic energy stored in bubble-walls:

$$E_{\text{kin}} = \kappa_\nu \cdot 4\pi \int_{t_n}^{t_p} dt \frac{dR}{dt}(t, t_n) R^2(t, t_n) \epsilon(t)$$

- $\epsilon(t)$: latent heat ($\sim$ vacuum energy)
- κ_ν: fraction of energy going into the wall motion (vs. heating the plasma)

Bubbles properties at collision

By definition:

- most bubbles collide at t_p
- majority of them produced at t_n

$\Rightarrow$ bubble physical radius: $\bar{R} = a(t_p) r(t_p, t_n)$

Kinetic energy stored in bubble-walls:

$$E_{\text{kin}} = \kappa_\nu \cdot 4\pi \int_{t_n}^{t_p} dt \frac{dR}{dt}(t, t_n) R^2(t, t_n) \epsilon(t)$$

- $\epsilon(t)$: latent heat ($\sim$ vacuum energy)
- κ_ν: fraction of energy going into the wall motion (vs. heating the plasma)

$\bar{R}$ and E_{kin}: key parameters to deduce the GW spectrum

Some assumptions

Entire dynamics specified by $\Gamma(t)$, $\epsilon(t)$, κ_ν, $v(t)$ and $a(t)$.

Some assumptions

Entire dynamics specified by $\Gamma(t)$, $\epsilon(t)$, κ_v, $v(t)$ and $a(t)$.

Very strong PT:

- large amount of vacuum energy released
- $\Rightarrow \kappa_v \sim 1$ [A. Kobakhidze et al, arXiv:1607.00883]
- $\Rightarrow v \sim 1$ (runaway bubbles) [C. Caprini et al., JCAP 1604 (2016) no.04 001]

Some assumptions

Entire dynamics specified by $\Gamma(t)$, $\epsilon(t)$, κ_ν, $v(t)$ and $a(t)$.

Very strong PT:

- large amount of vacuum energy released
- $\Rightarrow \kappa_\nu \sim 1$ [A. Kobakhidze et al, arXiv:1607.00883]
- $\Rightarrow v \sim 1$ (runaway bubbles) [C. Caprini et al., JCAP 1604 (2016) no.04 001]

Consider a radiation-dominated Universe:

- $a(t) \propto t^{1/2}$
- $t = \left(\frac{45 M_p^2}{16\pi^3 g_\star}\right)^{1/2} \frac{1}{T^2}$

Numerical results

Probability $p(T)$:

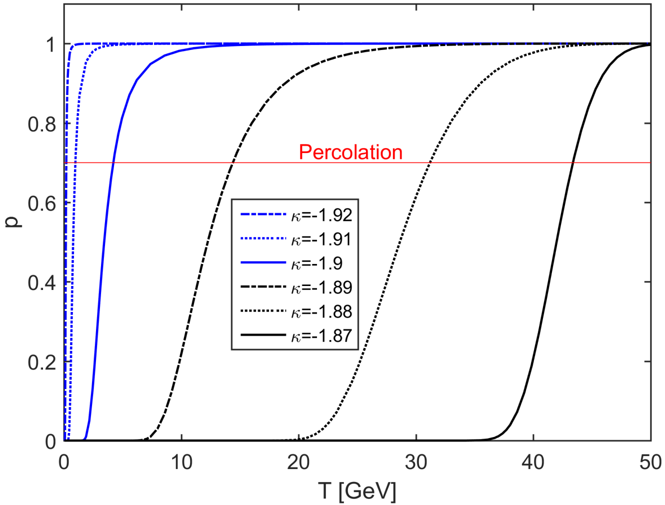

Numerical results

Number density distribution for $|\bar{\kappa}| = 1.9$: $\Rightarrow T_n \sim 49$ GeV

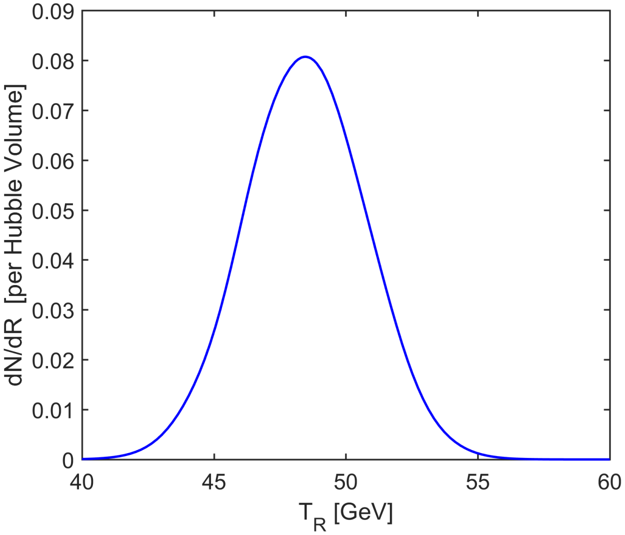

Numerical results

$\kappa\ [m_h^2/\lvert v\rvert]$	$T_\star$ GeV	T_n GeV	T_p GeV	$(\bar{R}H_p)^{-1}$	$\rho_{\text{kin}}/\rho_{\text{rad}}$
-1.87	85.9	48.9	43.4	8.79	0.57
-1.88	85.5	48.9	31.2	2.76	1.88
-1.89	84.5	49.0	14.4	1.41	37.8
-1.9	84.1	48.7	4.21	1.09	$5.09 \cdot 10^3$
-1.91	83.9	48.6	0.977	1.02	$1.73 \cdot 10^6$
-1.92	83.3	48.5	0.205	1.00	$8.80 \cdot 10^8$

Observations:

- new feature: $T_p \ll T_n$
- Hubble-size bubbles at collision
- $\rho_{\text{rad}} \ll \rho_{\text{kin}}$: confirm very strong scenario

GW spectra: results

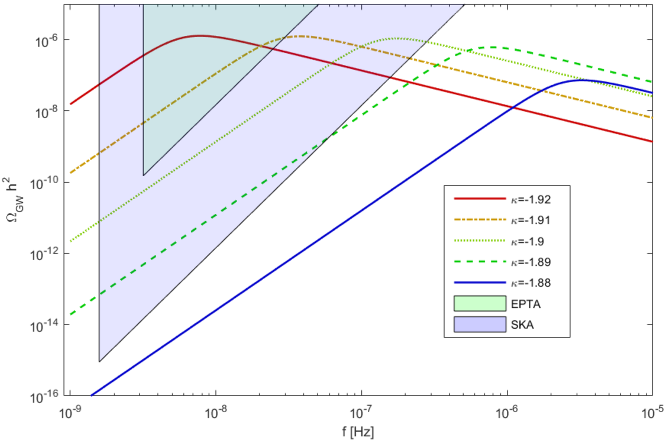

- Current constraints: EPTA, PPTA, NANOGrav
- Possible detection: Square Kilometre Array

[Moore et al., Class. Quant. Grav. 32 (2015) 015014]

Summary of Part II

- Stochastic background of GWs as a signature of new physics

- Different possible scenarios of 1st-order transitions:
  - standard electroweak transition at $T \sim 100$ GeV $\Rightarrow$ signal in LISA
  - prolonged electroweak transition $\Rightarrow$ signal in PTA

- Not limited to the model discussed here

General Conclusion

- The detection of Gravitational Waves represents a milestone by itself.

General Conclusion

- The detection of Gravitational Waves represents a milestone by itself.
- It also provides new opportunities to probe various area of fundamental physics from General Relativity to Particle Physics.

General Conclusion

- The detection of Gravitational Waves represents a milestone by itself.
- It also provides new opportunities to probe various area of fundamental physics from General Relativity to Particle Physics.
- There are lot of expectations regarding the future experiments like KAGRA, LISA, SKA, etc

Backup slides

Standard Model with hidden scale invariance

- Scale invariant models are attractive to address the hierarchy problem

  e.g.: [K. Meissner, H. Nicolai, PLB 648 (2007) 312] [R. Foot et al., PRD 77 (2008) 035006] [S. Iso et al., PLB 676 (2009) 81]

Standard Model with hidden scale invariance

- Scale invariant models are attractive to address the hierarchy problem

  e.g.: [K. Meissner, H. Nicolai, PLB 648 (2007) 312] [R. Foot et al., PRD 77 (2008) 035006] [S. Iso et al., PLB 676 (2009) 81]

- Assume existence of UV complete scale invariant model (string theory,...)

Standard Model with hidden scale invariance

- Scale invariant models are attractive to address the hierarchy problem

  e.g.: [K. Meissner, H. Nicolai, PLB 648 (2007) 312] [R. Foot et al., PRD 77 (2008) 035006] [S. Iso et al., PLB 676 (2009) 81]

- Assume existence of UV complete scale invariant model (string theory,...)
- Focus on low-energy effective field theory:
  - Standard Model Higgs potential at UV scale Λ

$$V(\Phi^\dagger\Phi) = V_0(\Lambda) + \lambda(\Lambda)\left[\Phi^\dagger\Phi - v_{ew}^2(\Lambda)\right]^2 + \ldots$$

  - spontaneously broken scale invariance manifests through dilaton field χ

$$\begin{aligned} \Lambda &\to \Lambda\frac{\chi}{f_\chi} \equiv \alpha\chi \\ v_{ew}^2(\Lambda) &\to \frac{v_{ew}^2(\alpha\chi)}{f_\chi^2}\chi^2 \equiv \frac{\xi(\alpha\chi)}{2}\chi^2 \\ V_0(\Lambda) &\to \frac{V_0(\alpha\chi)}{f_\chi^4}\chi^4 \equiv \frac{\rho(\alpha\chi)}{4}\chi^4 \end{aligned}$$

Standard Model with hidden scale invariance

- Scale invariant models are attractive to address the hierarchy problem

  e.g.: [K. Meissner, H. Nicolai, PLB 648 (2007) 312] [R. Foot et al., PRD 77 (2008) 035006] [S. Iso et al., PLB 676 (2009) 81]

- Assume existence of UV complete scale invariant model (string theory,...)
- Focus on low-energy effective field theory:
  - Standard Model Higgs potential at UV scale Λ

$$V(\Phi^\dagger\Phi) = V_0(\Lambda) + \lambda(\Lambda)\left[\Phi^\dagger\Phi - v_{ew}^2(\Lambda)\right]^2 + \ldots$$

  - spontaneously broken scale invariance manifests through dilaton field χ

$$\Lambda \to \Lambda\frac{\chi}{f_\chi} \equiv \alpha\chi$$
$$v_{ew}^2(\Lambda) \to \frac{v_{ew}^2(\alpha\chi)}{f_\chi^2}\chi^2 \equiv \frac{\xi(\alpha\chi)}{2}\chi^2$$
$$V_0(\Lambda) \to \frac{V_0(\alpha\chi)}{f_\chi^4}\chi^4 \equiv \frac{\rho(\alpha\chi)}{4}\chi^4$$

We get an effective scale invariant potential:

$$V(\Phi^\dagger\Phi,\chi) = \lambda(\alpha\chi)\left[\Phi^\dagger\Phi - \frac{\xi(\alpha\chi)}{2}\chi^2\right]^2 + \frac{\rho(\alpha\chi)}{4}\chi^4$$

Hierarchy and light dilaton

- Scale invariance is broken by quantum effects:

$$\lambda^{(i)}(\alpha\chi) = \lambda^{(i)}(\mu) + \beta_{\lambda^{(i)}}(\mu)\ln\left(\alpha\chi/\mu\right) + \beta'_{\lambda^{(i)}}(\mu)\ln^2\left(\alpha\chi/\mu\right) + \ldots$$

Hierarchy and light dilaton

- Scale invariance is broken by quantum effects:

$$\lambda^{(i)}(\alpha\chi) = \lambda^{(i)}(\mu) + \beta_{\lambda^{(i)}}(\mu) \ln(\alpha\chi/\mu) + \beta'_{\lambda^{(i)}}(\mu) \ln^2(\alpha\chi/\mu) + \ldots$$

- Minimisation conditions and small vacuum energy density:

$$\left.\frac{\partial V}{\partial \chi}\right|_{\Phi=v_{ew},\chi=v_\chi} = 0, \quad \left.\frac{\partial V}{\partial \Phi}\right|_{\Phi=v_{ew},\chi=v_\chi} = 0, \quad V(v_{ew}, v_\chi) = 0$$

Hierarchy and light dilaton

- Scale invariance is broken by quantum effects:

$$\lambda^{(i)}(\alpha\chi) = \lambda^{(i)}(\mu) + \beta_{\lambda^{(i)}}(\mu)\ln(\alpha\chi/\mu) + \beta'_{\lambda^{(i)}}(\mu)\ln^2(\alpha\chi/\mu) + \ldots$$

- Minimisation conditions and small vacuum energy density:

$$\left.\frac{\partial V}{\partial \chi}\right|_{\Phi=v_{ew},\chi=v_\chi} = 0, \quad \left.\frac{\partial V}{\partial \Phi}\right|_{\Phi=v_{ew},\chi=v_\chi} = 0, \quad V(v_{ew}, v_\chi) = 0$$

- We obtain dimensional transmutation and hierarchy of VEVs ($\Lambda \sim v_\chi$):

$$\rho(v_\chi) = 0, \quad \beta_\rho(v_\chi) = 0, \quad \xi(v_\chi) = \frac{v_{ew}^2}{v_\chi^2}$$

Hierarchy and light dilaton

- Scale invariance is broken by quantum effects:

$$\lambda^{(i)}(\alpha\chi) = \lambda^{(i)}(\mu) + \beta_{\lambda^{(i)}}(\mu)\ln(\alpha\chi/\mu) + \beta'_{\lambda^{(i)}}(\mu)\ln^2(\alpha\chi/\mu) + \ldots$$

- Minimisation conditions and small vacuum energy density:

$$\left.\frac{\partial V}{\partial \chi}\right|_{\Phi=v_{ew},\chi=v_\chi} = 0, \quad \left.\frac{\partial V}{\partial \Phi}\right|_{\Phi=v_{ew},\chi=v_\chi} = 0, \quad V(v_{ew}, v_\chi) = 0$$

- We obtain dimensional transmutation and hierarchy of VEVs ($\Lambda \sim v_\chi$):

$$\rho(v_\chi) = 0, \quad \beta_\rho(v_\chi) = 0, \quad \xi(v_\chi) = \frac{v_{ew}^2}{v_\chi^2}$$

- $\xi(v_\chi)$ can be hierarchically small (technical naturalness)

Hierarchy and light dilaton

- Scale invariance is broken by quantum effects:

$$\lambda^{(i)}(\alpha\chi) = \lambda^{(i)}(\mu) + \beta_{\lambda^{(i)}}(\mu)\ln(\alpha\chi/\mu) + \beta'_{\lambda^{(i)}}(\mu)\ln^2(\alpha\chi/\mu) + ...$$

- Minimisation conditions and small vacuum energy density:

$$\left.\frac{\partial V}{\partial \chi}\right|_{\Phi=v_{ew},\chi=v_\chi} = 0, \quad \left.\frac{\partial V}{\partial \Phi}\right|_{\Phi=v_{ew},\chi=v_\chi} = 0, \quad V(v_{ew}, v_\chi) = 0$$

- We obtain dimensional transmutation and hierarchy of VEVs ($\Lambda \sim v_\chi$):

$$\rho(v_\chi) = 0, \quad \beta_\rho(v_\chi) = 0, \quad \xi(v_\chi) = \frac{v_{ew}^2}{v_\chi^2}$$

- $\xi(v_\chi)$ can be hierarchically small (technical naturalness)
- Prediction of a light dilaton: $m_\chi^2 \simeq \frac{\beta'_\rho(v_\chi)}{4\xi(v_\chi)} v_{ew}^2 \qquad \frac{m_\chi}{m_h} \sim \sqrt{\xi}$

Recovering the Standard Model at $\mu = v_{ew}$

- Consider the running of parameters between v_{ew} and $v_\chi \sim \Lambda$

Recovering the Standard Model at $\mu = v_{ew}$

- Consider the running of parameters between v_{ew} and $v_\chi \sim \Lambda$
- Require that $m_\chi^2(v_{ew}) > 0$

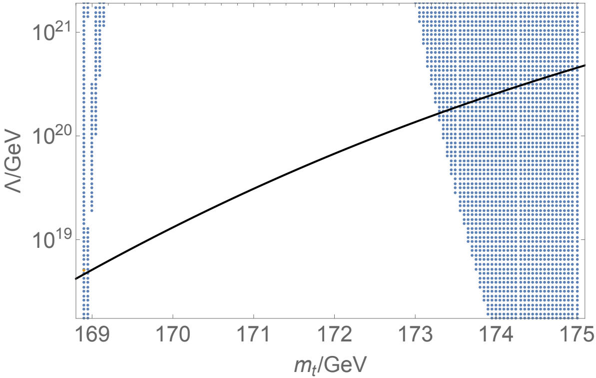

Recovering the Standard Model at $\mu = v_{ew}$

- Consider the running of parameters between v_{ew} and $v_\chi \sim \Lambda$
- Require that $m_\chi^2(v_{ew}) > 0$

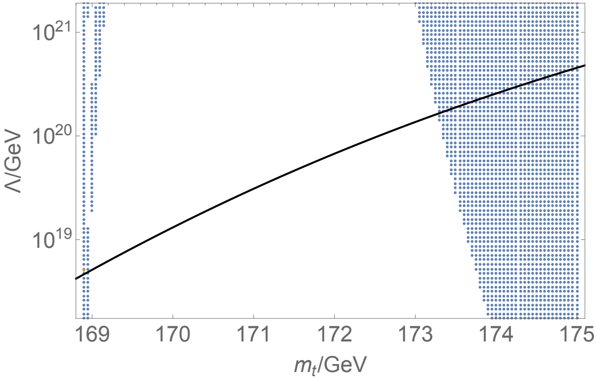

- Dilaton mass at $v_\chi \sim \Lambda \sim M_P$: $m_\chi \sim 10^{-8}$ eV

Recovering the Standard Model at $\mu = v_{ew}$

- Consider the running of parameters between v_{ew} and $v_\chi \sim \Lambda$
- Require that $m_\chi^2(v_{ew}) > 0$

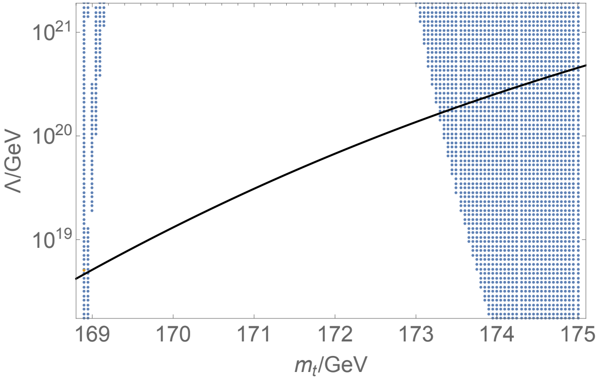

- Dilaton mass at $v_\chi \sim \Lambda \sim M_P$: $m_\chi \sim 10^{-8}$ eV
- Indicative only and requires higher-loop corrections

Electroweak and QCD phase transitions

In the Standard Model, both electroweak and QCD PTs are crossover

[K. Kajantie et al., Phys. Rev. Lett. 77 (1996) 2887] [Y. Aoki et al, Nature 443 (2006) 675]

$\Rightarrow$ no stochastic GW background predicted in the SM

Electroweak and QCD phase transitions

In the Standard Model, both electroweak and QCD PTs are crossover

[K. Kajantie et al., Phys. Rev. Lett. 77 (1996) 2887] [Y. Aoki et al, Nature 443 (2006) 675]

$\Rightarrow$ no stochastic GW background predicted in the SM

In the model with hidden scale invariance:

- flat direction in the Higgs-dilaton potential at tree level
- vacua are almost degenerate $\Rightarrow$ no EWPT until $T \ll T_{EW}$

Electroweak and QCD phase transitions

In the Standard Model, both electroweak and QCD PTs are crossover

[K. Kajantie et al., Phys. Rev. Lett. 77 (1996) 2887] [Y. Aoki et al, Nature 443 (2006) 675]

$\Rightarrow$ no stochastic GW background predicted in the SM

In the model with hidden scale invariance:

- flat direction in the Higgs-dilaton potential at tree level
- vacua are almost degenerate $\Rightarrow$ no EWPT until $T \ll T_{EW}$

QCD-induced electroweak phase transition:

- supercooling until $T \sim T_{QCD}$
- at T_{QCD}: chiral phase transition with 6 massless quarks
- quark condensates reduce the barrier in the Higgs potential $\Rightarrow$ EWPT

Electroweak and QCD phase transitions

In the Standard Model, both electroweak and QCD PTs are crossover

[K. Kajantie et al., Phys. Rev. Lett. 77 (1996) 2887] [Y. Aoki et al, Nature 443 (2006) 675]

$\Rightarrow$ no stochastic GW background predicted in the SM

In the model with hidden scale invariance:

- flat direction in the Higgs-dilaton potential at tree level
- vacua are almost degenerate $\Rightarrow$ no EWPT until $T \ll T_{EW}$

QCD-induced electroweak phase transition:

- supercooling until $T \sim T_{QCD}$
- at T_{QCD}: chiral phase transition with 6 massless quarks
- quark condensates reduce the barrier in the Higgs potential $\Rightarrow$ EWPT

See also: [E. Witten Nucl.Pys.B177 (1981) 477] [W. Buchmuller, D. Wyler, PLB 249 (1990) 281] [S. Iso et al., PRL 119 (2017) 141301] [B. von Harling, G. Servant, JHEP 1801 (2018) 159]

Thermal Higgs-dilaton potential + quark condensates

- Thermal contributions to the Higgs-dilaton potential ⇒ barrier along the flat direction:

$$V_T(h,\chi(h)) \approx AT^4 + \frac{1}{48}\left[4\lambda(\Lambda) + 6y_t^2(\Lambda) + \frac{9}{2}g^2(\Lambda) + \frac{3}{2}g'^2(\Lambda)\right] h^2T^2 + \dots$$

Thermal Higgs-dilaton potential + quark condensates

- Thermal contributions to the Higgs-dilaton potential $\Rightarrow$ barrier along the flat direction:

$$V_T(h,\chi(h)) \approx AT^4 + \frac{1}{48}\left[4\lambda(\Lambda) + 6y_t^2(\Lambda) + \frac{9}{2}g^2(\Lambda) + \frac{3}{2}g'^2(\Lambda)\right] h^2T^2 + \dots$$

- Quark-antiquark condensate with N massless quarks [J. Gasser, H. Leutwyler, PLB 184 (1987) 83] :

$$\langle\bar{q}q\rangle_T = \langle\bar{q}q\rangle\left[1-(N^2-1)\frac{T^2}{12Nf_\pi^2} - \frac{1}{2}(N^2-1)\left(\frac{T^2}{12Nf_\pi^2}\right)^2 + \dots\right]$$

Thermal Higgs-dilaton potential + quark condensates

- Thermal contributions to the Higgs-dilaton potential $\Rightarrow$ barrier along the flat direction:

$$V_T(h,\chi(h)) \approx AT^4 + \frac{1}{48}\left[4\lambda(\Lambda) + 6y_t^2(\Lambda) + \frac{9}{2}g^2(\Lambda) + \frac{3}{2}g'^2(\Lambda)\right] h^2T^2 + \dots$$

- Quark-antiquark condensate with N massless quarks [J. Gasser, H. Leutwyler, PLB 184 (1987) 83] :

$$\langle\bar{q}q\rangle_T = \langle\bar{q}q\rangle\left[1 - (N^2-1)\frac{T^2}{12Nf_\pi^2} - \frac{1}{2}(N^2-1)\left(\frac{T^2}{12Nf_\pi^2}\right)^2 + \dots\right]$$

- Quark-Higgs Yukawa interactions induce a linear term in the potential:

$$V_T(h) \to V_T(h) + \frac{y_q}{\sqrt{2}}\langle\bar{q}q\rangle_T h$$

Thermal Higgs-dilaton potential + quark condensates

- Thermal contributions to the Higgs-dilaton potential $\Rightarrow$ barrier along the flat direction:

$$V_T(h,\chi(h)) \approx AT^4 + \frac{1}{48}\left[4\lambda(\Lambda) + 6y_t^2(\Lambda) + \frac{9}{2}g^2(\Lambda) + \frac{3}{2}g'^2(\Lambda)\right] h^2T^2 + \ldots$$

- Quark-antiquark condensate with N massless quarks [J. Gasser, H. Leutwyler, PLB 184 (1987) 83] :

$$\langle\bar{q}q\rangle_T = \langle\bar{q}q\rangle\left[1-(N^2-1)\frac{T^2}{12Nf_\pi^2} - \frac{1}{2}(N^2-1)\left(\frac{T^2}{12Nf_\pi^2}\right)^2 + \ldots\right]$$

- Quark-Higgs Yukawa interactions induce a linear term in the potential:

$$V_T(h) \to V_T(h) + \frac{y_q}{\sqrt{2}}\langle\bar{q}q\rangle_T h$$

- This linear term dominates over the barrier for small enough T

Results and dynamics of the transitions

- For $N = 6$ and $f_\pi \approx 93$ MeV, $\langle \bar{q}q \rangle_{T_c} = 0$ at $T_c \approx 132$ MeV

Results and dynamics of the transitions

- For $N = 6$ and $f_\pi \approx 93$ MeV, $\langle \bar{q}q \rangle_{T_c} = 0$ at $T_c \approx 132$ MeV
- For $T \approx 127$ MeV the barrier disappears and the EWPT completes

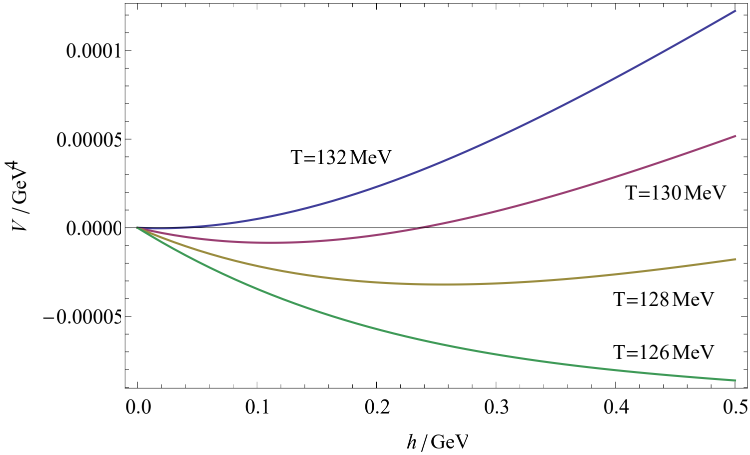

Results and dynamics of the transitions

- For $N = 6$ and $f_\pi \approx 93$ MeV, $\langle \bar{q}q \rangle_{T_c} = 0$ at $T_c \approx 132$ MeV
- For $T \approx 127$ MeV the barrier disappears and the EWPT completes
- The Higgs-dilaton rolls down the potential (smooth transition)

Results and dynamics of the transitions

- For $N = 6$ and $f_\pi \approx 93$ MeV, $\langle \bar{q}q \rangle_{T_c} = 0$ at $T_c \approx 132$ MeV
- For $T \approx 127$ MeV the barrier disappears and the EWPT completes
- The Higgs-dilaton rolls down the potential (smooth transition)
- However, $SU(6)_R \times SU(6)_L$ chiral symmetry breaking is 1st-order for massless quarks [D. Pisarski, F. Wilczek, PRD 29 (1984) 338]

Results and dynamics of the transitions

- For $N = 6$ and $f_\pi \approx 93$ MeV, $\langle \bar{q}q \rangle_{T_c} = 0$ at $T_c \approx 132$ MeV
- For $T \approx 127$ MeV the barrier disappears and the EWPT completes
- The Higgs-dilaton rolls down the potential (smooth transition)
- However, $SU(6)_R \times SU(6)_L$ chiral symmetry breaking is 1st-order for massless quarks [D. Pisarski, F. Wilczek, PRD 29 (1984) 338]
- Implicit assumption: chiral transition completes quickly

Results and dynamics of the transitions

- For $N = 6$ and $f_\pi \approx 93$ MeV, $\langle \bar{q} q \rangle_{T_c} = 0$ at $T_c \approx 132$ MeV
- For $T \approx 127$ MeV the barrier disappears and the EWPT completes
- The Higgs-dilaton rolls down the potential (smooth transition)
- However, $SU(6)_R \times SU(6)_L$ chiral symmetry breaking is 1st-order for massless quarks [D. Pisarski, F. Wilczek, PRD 29 (1984) 338]
- Implicit assumption: chiral transition completes quickly
- More refined analysis currently under investigation:
  - effective field theory for the Higgs, dilaton and pions
  - $U(6) \times U(6)$ linear sigma model for the pions

$$\mathcal{L} = \text{Tr}\left(\partial_\mu \varphi^\dagger \partial^\mu \varphi - m^2 \varphi^\dagger \varphi\right) - \lambda_1 \left[\text{Tr}\left(\varphi^\dagger \varphi\right)\right]^2 - \lambda_2 \text{Tr}\left(\varphi^\dagger \varphi\right)^2 + \mathcal{L}(\varphi, \phi, \chi)$$

  - requires a proper treatment of infrared divergences

Gravitational Waves

- 1st order chiral transition $\Rightarrow$ stochastic background of GWs

Gravitational Waves

- 1st order chiral transition $\Rightarrow$ stochastic background of GWs
- Peak frequency roughly given by duration of transition (size of bubbles at collision): $f_p \approx v R_c^{-1}$

Gravitational Waves

- 1st order chiral transition $\Rightarrow$ stochastic background of GWs
- Peak frequency roughly given by duration of transition (size of bubbles at collision): $f_p \approx v R_c^{-1}$
- observed frequency today:

$$f_0 = f_p \frac{a(t_c)}{a(t_0)} \approx 1.65 \cdot 10^{-8} \frac{v}{R_c\, H_c} \frac{T_c}{100 \text{ MeV}} \text{ Hz} \approx 10^{-7} \text{ Hz}$$

Gravitational Waves

- 1st order chiral transition $\Rightarrow$ stochastic background of GWs
- Peak frequency roughly given by duration of transition (size of bubbles at collision): $f_p \approx v R_c^{-1}$
- observed frequency today:

$$f_0 = f_p \frac{a(t_c)}{a(t_0)} \approx 1.65 \cdot 10^{-8} \frac{v}{R_c\, H_c} \frac{T_c}{100 \text{ MeV}} \text{ Hz} \approx 10^{-7} \text{ Hz}$$

- possible detection with Pulsar Timing Arrays (EPTA, NANOGrav, SKA)

[C. Caprini et al., PRD 82 (2010) 063511] [A. Kobakhidze et al., EPJ C77 (2017) 570]

Gravitational Waves

- 1st order chiral transition $\Rightarrow$ stochastic background of GWs
- Peak frequency roughly given by duration of transition (size of bubbles at collision): $f_p \approx v R_c^{-1}$
- observed frequency today:

$$f_0 = f_p \frac{a(t_c)}{a(t_0)} \approx 1.65 \cdot 10^{-8} \frac{v}{R_c\, H_c} \frac{T_c}{100\ \text{MeV}}\ \text{Hz} \approx 10^{-7}\ \text{Hz}$$

- possible detection with Pulsar Timing Arrays (EPTA, NANOGrav, SKA)

[C. Caprini et al., PRD 82 (2010) 063511] [A. Kobakhidze et al., EPJ C77 (2017) 570]

- precise spectrum and amplitude of the background currently under computation (within linear sigma model)

Gravitational Waves

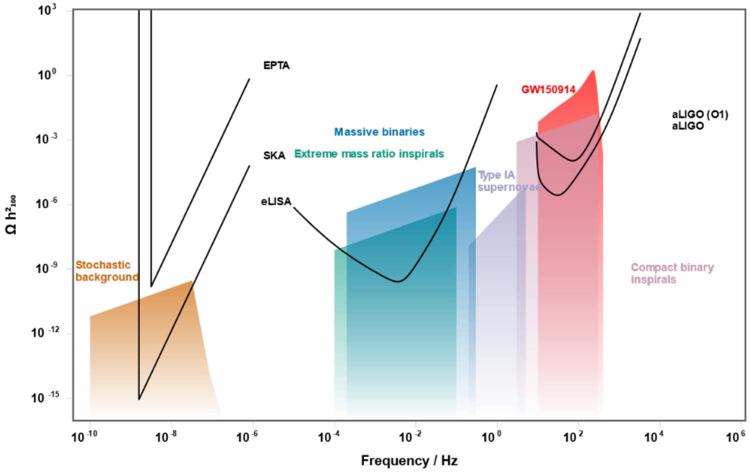

[From rhcole.com/apps/GWplotter/]

Summary of Backup

- Scale invariant extensions of the SM motivated by the hierarchy problem

Summary of Backup

- Scale invariant extensions of the SM motivated by the hierarchy problem
- Low energy effective formulation with a dilaton field

Summary of Backup

- Scale invariant extensions of the SM motivated by the hierarchy problem
- Low energy effective formulation with a dilaton field
- Interesting predictions:
  - small dilaton mass: $m_\chi \approx 10^{-8}$ eV
  - low temperature QCD-induced electroweak transition
  - potential GW signal in the range of Pulsar Timing Arrays

Summary of Backup

- Scale invariant extensions of the SM motivated by the hierarchy problem
- Low energy effective formulation with a dilaton field
- Interesting predictions:
  - small dilaton mass: $m_\chi \approx 10^{-8}$ eV
  - low temperature QCD-induced electroweak transition
  - potential GW signal in the range of Pulsar Timing Arrays
- To investigate further:
  - precise dynamics of the transitions
  - Black Holes production